

RESEARCH ARTICLE



ISSN: 2321-7758

A New Resonant Modular Multilevel Step down DC–DC Converter for Induction Motor Drive Application

J.V.S.E Narasinga Rao¹, B. Venugopal Reddy²

¹PG Scholar, Dept of EEE, Sri Venkateswara Engineering College, Suryapet, TS, India.

²Associate Professor, Dept of EEE, Sri Venkateswara Engineering College, Suryapet, TS, India



J.V.S.E NARASINGA RAO



B. VENUGOPAL REDDY

ABSTRACT

A modular multilevel converter (MMC) is one of the next-generation multilevel converters intended for high- or medium-voltage power conversion without transformers. The MMC is based on cascade connection of multiple bidirectional chopper-cells per leg, thus requiring voltage-balancing control of the multiple floating dc capacitors. MMCs require a complicated balancing control to maintain the voltage levels. Modular multilevel converters (MMCs) provide more than two levels which can be adjusted by changing the number of modular cells. Cells with a fault can also be bypassed while keeping the converters operating. High reliability and modularity are the main features of MMC. The modular multilevel converter (MMC) has very high importance in medium and high-voltage applications. Power electronics transformer can be used for high step-down ratio dc–dc power conversion, with high power rating and efficiency achieved. But this requires a large number of high isolation voltage transformers and a complicated balancing control scheme. The new MMC can achieve high step-down ratio depending on the number of sub modules and voltage balancing is very simple. The converter also exhibits simplicity and scalability with no necessary requirement of high-voltage isolation transformers. Resonant conversion is achieved between the series inductor and sub module capacitors. The proposed converter is applied for agriculture field induction motor application This new MMC is simulated using MATLAB/Simulink.

Keywords: DC–DC Conversion, Modular Multilevel Converters (MMCS), Phase-Shift Control, Resonant Converter, Step-Down Ratio.

©KY PUBLICATIONS

I. INTRODUCTION

Modular multilevel converters (MMCs) are used for dc–ac [1], ac–dc [4], ac–ac [9], and dc–dc conversion for medium-voltage and high-voltage applications. These converters provide more than two levels which can be adjusted by changing the number of modular cells. Cells with a fault can also be bypassed while keeping the converters operating. High reliability and modularity are the main features of MMCs. However, all these MMCs require a complicated balancing control to maintain

the voltage levels. Even though a requirement is placed on the tolerance of the cell capacitors, measuring capacitor voltages for balancing control is indispensable. Moreover, the operating frequency of the conventional control for MMCs is not higher than the switching frequency. High switching frequencies are used to reduce the sizes of passive components. Tradeoffs between switch ratings and converter size should be made, but it is hard to find a good solution for high-voltage, high-step-down ratio, and low-power applications. Other new multilevel modular switched capacitor dc–dc

converters designed for small-power applications are proposed in [14]. These converters exhibit good efficiency and modularity, but are not suitable for high-voltage applications. For high-voltage applications, conventional diode clamped, flying capacitor, or other types of converters are also not suitable as the circuit Configuration becomes quite complicated with increased number of levels. These converters have poor modularity and reliability. The most promising solution may be converters known as power electronics transformers (PETs) [11].

PETs are designed for high-power applications. They require a large number of transformers with high-voltage isolation. The isolation between the primary side and secondary side has to withstand the entire high input voltage, even if the voltage across the primary side is only a small fraction of this. The secondary side terminals of the transformers are connected in parallel, and the balancing control between modules is necessary. PETs can be used for high-voltage and high-power applications with high efficiency, but the converter size will be increased dramatically with a high-voltage step down ratio. Therefore, other simple solutions may be promising for low-power applications in medium-voltage and high-voltage applications. This paper presents a new form of MMC for high-voltage step-down unidirectional dc-dc conversion [13]. The proposed converter has inherent-balancing of each capacitor voltage. High step-down voltage conversion ratios can be achieved by using large numbers of sub modules. With phase-shifted pulse width-modulation (PWM), higher operating frequency can also be achieved [16]. Which is equivalent to the product of the number of sub modules and the switching frequency. Moreover, the converter operates with two resonant frequencies where zero voltage-switching (ZVS) and/or zero-current-switching (ZCS) become possible. The proposed converters are more suitable for low-power dc-dc applications as it has the feature of modularity, simplicity, and flexibility. The detailed configuration and operation principle are presented, and verified by experimental results from bench-scale prototype tests.

II. HIGH STEP-DOWN RATIO DC-DC CONVERTERS AND GENERAL OPERATING PRINCIPLE

A. System Configuration

In [13], a family of dc-dc converters are discussed in which three groups of sub modules are used as two voltage dividers, and passive filters are provided at input and outputs connections to pass and block currents of appropriate frequencies. On the right-half-hand side of the circuit in one load is fed by one group of sub modules.

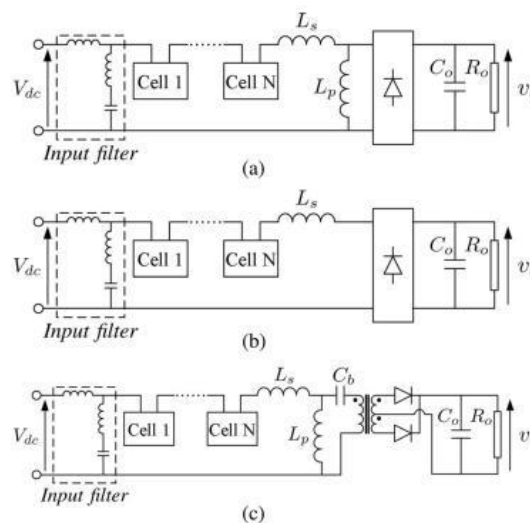


Fig.1.High step-down ratio unidirectional dc-dc converter topologies (a) Transformer less converter with series-parallel resonance. (b) Transformer less converter with series resonance. (c) Transformer isolated converter.

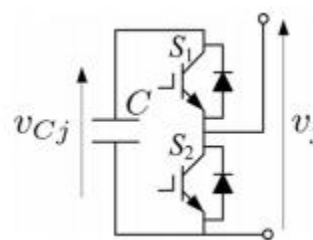


Fig.2. Circuit configuration of a half-bridge cell.

Here, the proposal is also to use only one group of sub modules in the upper position to support the dc-voltage difference between the input and output but also provide excitation to a resonant output stage connected to the return terminal of the input. Fig. 1(a) and (b) shows series-parallel and series resonant versions in which the resonance is between the series inductors and the sub module capacitors. The sub modules are illustrated in Fig. 2. The output rectifier can be coupled via a

transformer but only by adding a capacitor to block the dc current as shown in Fig. 1(c). For the circuits of Fig. 1(a) and (c), the dc current drawn from the input and through the cells returns via the parallel inductor L_p . For the circuit of Fig. 1(b), where this path is absent, the return of the dc input current is via the rectifier and load.

B. Phase-Shifted PWM for High Step-Down Ratio

To support the input voltage, the sub modules of Fig1 are used predominantly in the “one state” in which the upper switch is ON and the module inserts the capacitor voltage into the circuit. Phase-shifted PWM is then applied with a high duty-ratio such that an excitation is applied to the resonant components. The effective frequency of this excitation is much higher than the frequency of switching of an individual cell. This is arranged so that only one cell at a time is in “zero state,” and thus, the step-down ratio of the circuit becomes dependent on the number of cells N . To demonstrate the general operation principle, the converter in Fig. 1(a) with five half-bridge cells is used as an example. Fig. 3 shows the circuit diagram with the input filter removed to simplify the analysis. The dc input voltage is V_{dc} . The capacitor voltage and output voltage of j th ($j = 1,2,...,5$) cell are represented by v_{Cj} and v_j , respectively. The input current is composed of the dc component and ac component. The dc current component returns to the converter input mainly through the parallel inductor L_s , where an ac current component mainly flows to the rectifier.

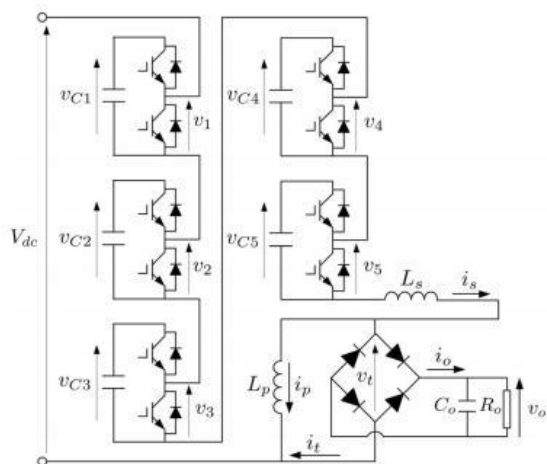


Fig.3. Five-cell step-down series-parallel resonant converter

The sum of the parallel inductor current i_p and the rectifier input current it is equal to i_s . The output current i_{on} is rectified from it. The switching frequencies and duty-ratios of cells are equal, but the PWM signals from Cell 1 to Cell 5 are shifted by $0^\circ, 72^\circ, 144^\circ, 216^\circ,$ and 288° , respectively. To analyze the circuit operation, the following assumptions are made:

- The switches are lossless and the cells are identical with the same parameters.
- The cutoff frequency of the input filter is much lower than the series current frequency in the converter. The input ac current and dc current flow through the parallel branch and the series branch of the input filter, respectively.
- The dc voltages of the cell capacitors are balanced at a steady state.
- The rectifier diodes are synchronously switched ON with the rectifier input voltage.

When the converter is operating at a steady state, the switching frequency is f_s and the duty-ratio of each cell is 90%. Based on the previous assumptions, the key voltage waveforms of the converter are shown in Fig. 4. With the phase-shift control, the output voltage of j th cell v_j is square wave ranging from 0 to the steady-state cell capacitor voltage v_{Cj} . Define output voltage across all the cells as $v_s = \sum_{j=1}^N v_j$. Therefore, v_s is ranging from the sum of four cells’ capacitor voltages to the sum of five cells’ capacitor voltages.

As all the cell capacitor voltages are assumed to be equal to v_C , the stack voltage v_s is comprised of a square wave ripple with the amplitude of $0.5v_C$ and a dc offset of $4.5v_C$. It can be observed from Fig. 4 that the ripple frequency is five times of the switching frequency. Assume there is no ac voltage drop across the passive components, the rectifier input voltage v_t is a square wave with the amplitude of $0.5v_C$ but in an opposite phase compared to the ripple of v_s . As the dc offset of v_s is $4.5v_C$ with $N = 5$, the cell capacitor voltage can be derived as $v_C = V_{dc}/4.5$.

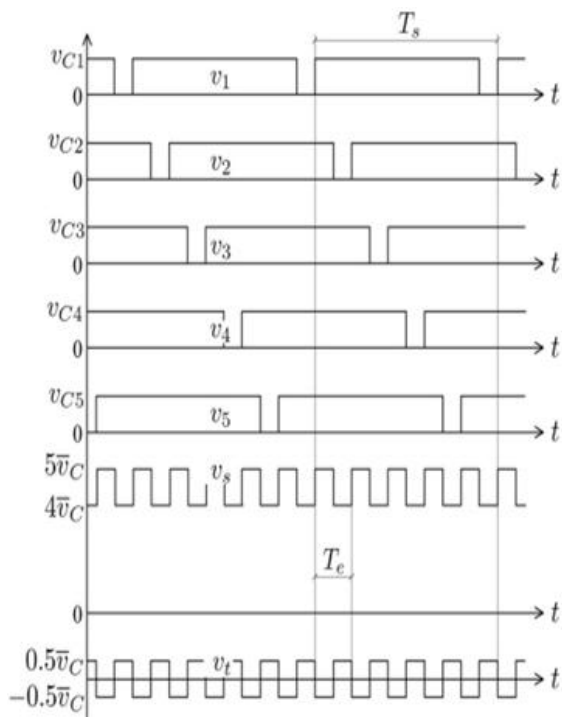


Fig.4. Time-domain key voltage waveforms of the five-cell converter

In a more general case with N cells, the average cell capacitor voltage can be derived as

$$\bar{v}_C = \frac{2V_{dc}}{2N - 1} \quad (1)$$

With the phase-shift angle of 360° and the duty-ratio of $2N - 1$. Hence, the peak voltage value of v_t is $0.5V_C$. If the converter output voltage v_o is close to the peak input voltage of the rectifier, this converter achieves a step-down ratio of $2N - 1$, which is a function of the number of half-bridge cells. With more cells in the converter, higher step-down voltage ratio can be achieved. The equivalent operating frequency f_e is expressed by

$$f_e = N f_s \quad (2)$$

Which is used to choose the passive components for the resonant operation.

Assume that the dc component and root mean square (RMS) value of an ac component of the series current are I_{dc} and I_{ac} , respectively. If we neglect the losses of the converter, the input power is almost equal to the output power, which can be written as

$$V_{dc} I_{dc} = \bar{v}_o I_{ac} \quad (3)$$

As $V_{dc}/v_o = 2N - 1$, it can be derived from (3) that $I_{ac} = (2N - 1)I_{dc}$. With a rated power P, the RMS of the ac current can be derived as

$$I_{ac} = (2N - 1)P/V_{dc} \quad (4)$$

This means that when the output power is constant, the current RMS value and switch stress are proportional to the step-down ratio. As the ac current is usually much higher than the dc current, the conduction losses mainly come from the ac current. If we assume that the average voltages across IGBTs and diodes are the same as V_{semi} , the conduction losses caused by the ac current can be written as

$$P_{ac} = I_{ac} V_{semi} N \quad (5)$$

Therefore, comparing P_{ac} to the input power, it can be derived that the efficiency η is limited by the conduction losses as

$$\eta < 1 - \frac{N(2N - 1)V_{semi}}{V_{dc}} \quad (6)$$

In most cases, if the current flowing through semiconductors is increased, the voltage drop on semiconductors increases. This gives a higher V_{semi} and the efficiency will reduce. As a result, the converter is only suitable for high-voltage and low-power applications. It can be seen from (6) that with a higher step down ratio, the efficiency reduces significantly. Therefore, the step-down ratio achieved by cells should be limited. In high voltage applications, IGBTs connected in series can also be used to construct a half-bridge. An isolation transformer can be used to further increase the step-down ratio without increasing the series ac current. Under such condition, the topology of Fig. 1(c) involving a step-down transformer becomes a good solution.

C. Resonant Operation and Inherent-Balancing

The converter family can operate in a resonant mode. The resonant operation of the converter in Fig. 1(a) is similar to that of classic series-parallel resonant converters. The operation principle of the converter in Fig. 1(b) is similar to that of series resonant converters. The resonant converter in Fig. 1(c) contains a dc-blocking capacitor and a transformer. With a relatively big capacitance C_b and magnetizing inductance of the transformer compared to that of the resonant tank, this converter can operate in a similar way to that of the converter in Fig. 1(a). This provides a further step-down voltage ratio without increasing the series current. This section presents the analysis of

the equivalent operation of the first configuration (see Fig. 3). The operation principle of other configurations can be analyzed by using the similar method. To demonstrate the operation principle in a simple way, the starting point is selected at the time when the capacitor of Cell 1 is involved into the resonant operation and the end point is selected at the time when capacitor of Cell 2 is out of the resonance. The relevant time interval can be found in Fig. 4 which is marked by the equivalent operating cycle T_e . Note that fixed dead time is used for all switches. Considering operation mode with dead band, there are four operation modes in each operating cycle, which are shown in Fig5. To analyze the circuit operation, we assume the parallel current i_p is above zero. The first mode starts when the lower switch in Cell 1 is turned OFF, and the circuit enters the dead time mode.

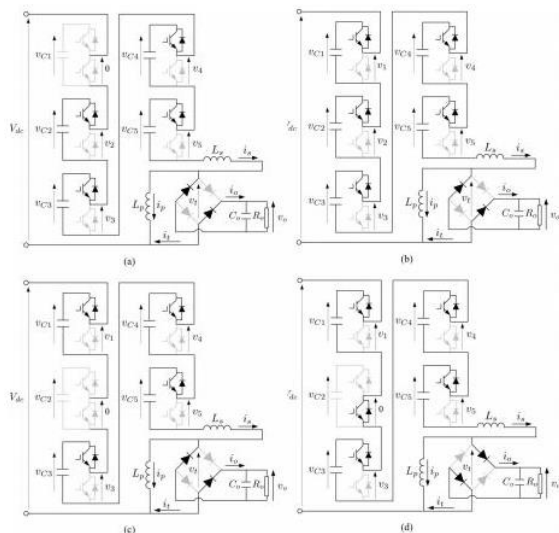


Fig.5. Operation modes in the first equivalent operating cycle. (a) Mode 1. (b) Mode 2. (c) Mode 3. (d) Mode 4. (black: on path; grey: off path) of Cell 1 [see Fig. 5(a)].

In this mode, no current flows through cells and all the current circulates between the parallel inductor and the rectifier. After a short time, the upper switch in Cell 1 is turned ON and the circuit enters mode 2 [see Fig. 5(b)]. All the cell capacitors are in series with the inductor L_s . The input voltage of the rectifier is negative. Therefore, the input current it is negative. This mode lasts until the upper switch of Cell 2 is turned OFF. Then, the circuit enters mode 3 [see Fig. 5(c)]. This mode is the dead time mode of Cell 2. As there is no series current, all

the current on the parallel inductor flows to the diode rectifier. Shortly after that, the lower switch of Cell 2 is turned ON and the circuit becomes another resonant circuit only with capacitors of Cells 1, 3, 4, and 5 in series with L_s [see Fig. 5(d)]. As v_t becomes positive in this mode, the series current starts to rise with its resonant waveform. In the second mode, where five capacitors are in series, the input voltage of the rectifier is negative ($v_t < 0$). With the resonant current flowing through relevant diodes, v_t is clamped by the output voltage as $v_t = -v_o$. If the output current does not fall to zero before the half T_e , the converter is operating in the continuous conduction mode (CCM). Otherwise, it may operate in the discontinuous conduction mode (DCM). When i_o falls to zero, the output is disconnected from the parallel inductor L_p and v_t is dependent on the current i_p until the next switching action occurs. On the other hand, in the last mode, one capacitor is out and four capacitors join the series resonance.

The input voltage of the rectifier is clamped as $v_t = v_o$ as long as the converter operates in the CCM. If i_o falls to zero before this half operating cycle, the operation mode becomes the DCM and $i_s = i_p$ until the end of this operating cycle. In the next cycle T_e , the capacitor of Cell 2 will be in, and later on, the capacitor of Cell 3 will be out. The following capacitors' in and out sequence should be the capacitors of

Cell 3 and Cell 4, the capacitors of Cell 4 and Cell 5, the capacitors of Cell 5 and Cell 1, and finally back to the capacitors of Cell 1 and Cell 2 in the next switching cycle. Hence, there are always five capacitors or four capacitors in the series resonant operation alternatively, with the duration of each mode as half T_e . The total voltage on the series capacitors is always clamped through the diode bridge by the constant output voltage and the input voltage.

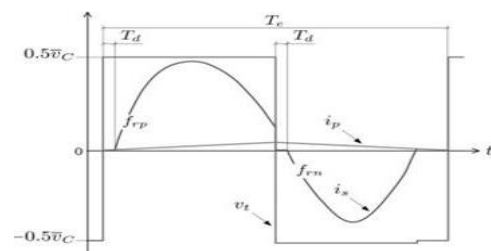


Fig.6. Time-domain waveforms of the resonant tank

Therefore, the dc voltages of all the capacitors should be equal in the steady state. This gives the inherent-balancing ability of the cell capacitors during the series operation.

When there are five capacitors in, the resonant tank is formed by five capacitors in series with L_s . When there are four capacitors in, the resonant tank is formed by four capacitors in series with L_s . Therefore, two resonant frequencies exist in the operation. Furthermore, for a general converter, the resonant frequency in the negative half-cycle is written as

$$f_{rn} = \frac{1}{2\pi\sqrt{L_s C/N}} \tag{7}$$

The resonant frequency in the positive half-cycle is

$$f_{rp} = \frac{1}{2\pi\sqrt{L_s C/(N-1)}} \tag{8}$$

As $f_{rp} < f_{rn}$, f_{rp} and f_{rn} are defined as the first resonant frequency and the second resonant frequency, respectively. The resonant tank waveforms of the proposed converter when using an operating frequency between f_{rp} and f_{rn} are shown in Fig. 6. Here, a low dc current plus an ac current on the parallel inductor are assumed. Note that this converter is operating differently to the classic LLC resonant converters [22] as two resonant frequencies exist during an operation cycle. In the case of Fig. 6, as in the positive half-cycle $f_e > f_{rp}$, the series current resonates with frequency of f_{rp} and the converter operates in the CCM. In the negative half-cycle $f_e > f_{rn}$, the series current resonates with frequency of f_{rn} and the converter operates in the DCM. There are five operating cycles in each switching cycle. Therefore, based on Fig. 6, the voltages and currents of the two switches in any cell can be obtained in Fig. 7. Note that when a switch is OFF, the current is zero. It can be seen that the converter can achieve ZCS and ZVS for the upper switches, but it cannot achieve soft switching for the lower switches. The turn-off current of the lower switch is high because the operating frequency is higher than the second resonant frequency f_{rn} . In general, ZCS cannot be achieved for any switch if the operating frequency is higher than the second resonant frequency f_{rn} as shown in Fig.8. On the other hand, if the operating frequency is lower than the first resonant frequency f_{rp} , ZCS and ZVS for

upper switches and near ZCS and near ZVS for lower switches are achieved.

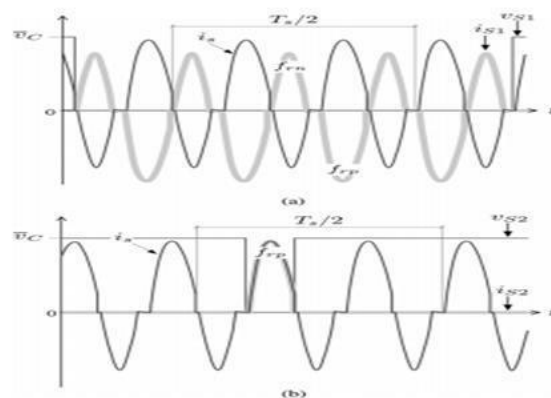


Fig.7. Time-domain waveforms of the voltages and currents of the cell switches (a) Upper switch. (b) Lower switch

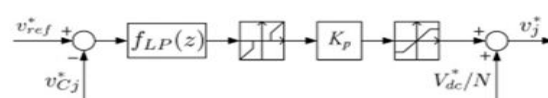


Fig.8. Voltage controller of each cell

However, the low operating frequency results in high conducting peak current. For most IGBTs, as both the collector-emitter saturation voltage and diode forward voltage increase significantly if the current increases, higher peak current may lead to higher conduction losses. Meanwhile, the stress on devices is also increased. On the other hand, when the switching frequency increases, switching losses will increase significantly due to the increased times of switching actions. Therefore, a good tradeoff according to a practical converter should be made to minimize the total losses. Note that the resonant operation with inherent-balancing of the converter is achieved using a diode rectifier. Thus, the converter topology can only provide unidirectional power flow. The bidirectional operation may be achieved using an active rectifier instead. However, as an active rectifier has three different voltage levels on its ac input side, implementing active voltage clamping for cell capacitor balancing is difficult. This converter topology would require a new control scheme and a different operation method.

Table I: Parameters of the Two Converter Schemes

Scheme	Side	Device voltage	Device current	Module number	IGBT/Diode applicable
ISOP DAB	Input	2000 V	10 A	5	SSNG 0250P330305×10
	Output	800 V	25A	5	DSEP60-12AR×20
Proposed	Input	2223 V	125 A	5	SSNG 0250P330305×10
	Output	800 V	125 A	1	DSEP60-12AR×20

Table II: Parameters of the Experimental System

Symbol	Quantity	Value
P	Rated power	250 W
V_{dc}	Nominal input dc voltage	500 V
v_o	Output dc voltage	45 V
I_{pk}	Maximum switch current	30 A
T_b	Sampling period	1 ms
L_{in}	Input filter inductor	9.8 mH
C_{in}	Input filter capacitor	840 μ F
L_s	Series inductor	6.5 μ H
L_p	Parallel inductor	3.3 mH
C_1	Cell 1 capacitor	57.9 μ F
C_2	Cell 2 capacitor	69.1 μ F
C_3	Cell 3 capacitor	58.2 μ F
C_4	Cell 4 capacitor	57.7 μ F
C_5	Cell 5 capacitor	57.8 μ F
C_o	Output capacitor	3 mF

III. INDUCTION MOTOR (IM)

An induction motor is an example of asynchronous AC machine, which consists of a stator and a rotor. This motor is widely used because of its strong features and reasonable cost. A sinusoidal voltage is applied to the stator, in the induction motor, which results in an induced electromagnetic field. A current in the rotor is induced due to this field, which creates another field that tries to align with the stator field, causing the rotor to spin. A slip is created between these fields, when a load is applied to the motor. Compared to the synchronous speed, the rotor speed decreases, at higher slip values. The frequency of the stator voltage controls the synchronous speed. The frequency of the voltage is applied to the stator through power electronic devices, which allows the control of the speed of the motor. The research is using techniques, which implement a constant voltage to

frequency ratio. Finally, the torque begins to fall when the motor reaches the synchronous speed. Thus, induction motor synchronous speed is defined by following equation,

$$n_s = \frac{120f}{P} \tag{9}$$

Where f is the frequency of AC supply, n, is the speed of rotor; p is the number of poles per phase of the motor. By varying the frequency of control circuit through AC supply, the rotor speed will change.

A. Control Strategy of Induction Motor

Power electronics interface such as three-phase SPWM inverter using constant closed loop Volts I Hertz control scheme is used to control the motor. According to the desired output speed, the amplitude and frequency of the reference (sinusoidal) signals will change. In order to maintain constant magnetic flux in the motor, the ratio of the voltage amplitude to voltage frequency will be kept constant. Hence a closed loop Proportional Integral (PI) controller is implemented to regulate the motor speed to the desired set point. The closed loop speed control is characterized by the measurement of the actual motor speed, which is compared to the reference speed while the error signal is generated. The magnitude and polarity of the error signal correspond to the difference between the actual and required speed. The PI controller generates the corrected motor stator frequency to compensate for the error, based on the speed error.

IV. SIMULATION RESULTS

Simulation results of this paper is as shown in below Figs.9 to 16.

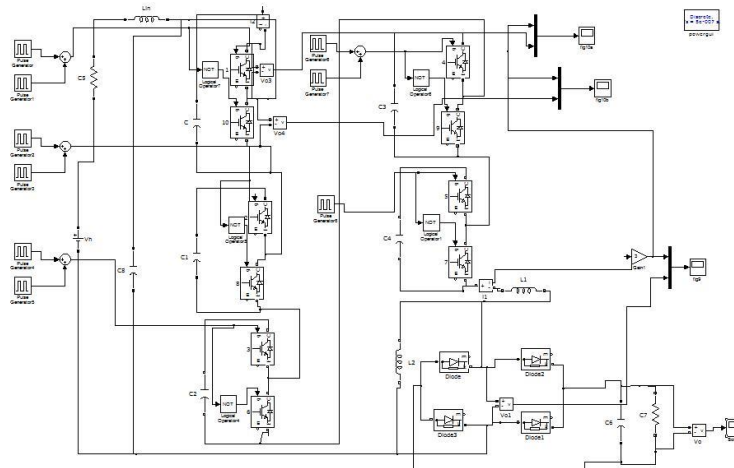


Fig 9 Matlab/simulation circuit of High step-down ratio unidirectional dc–dc converter topologies

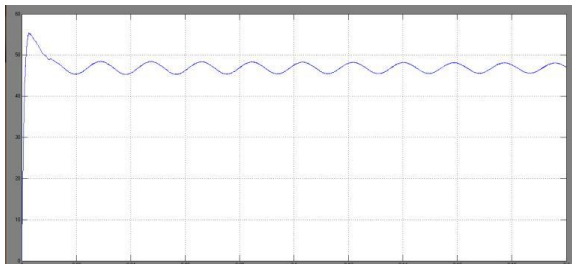
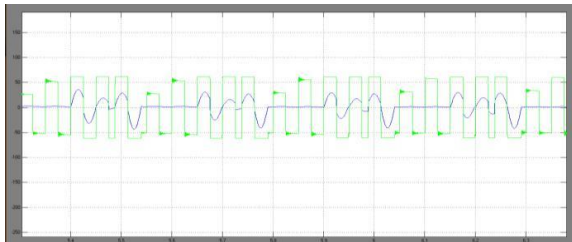
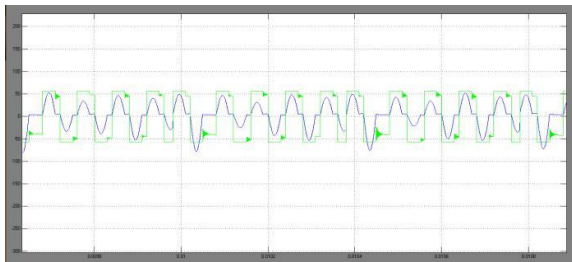


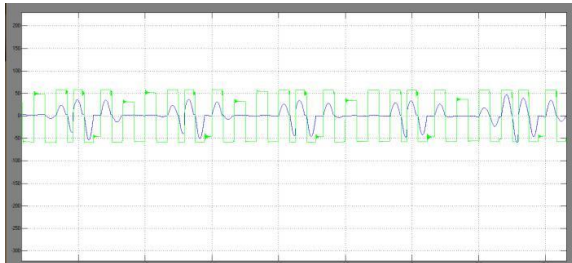
Fig.10. simulation wave form of high step-down ratio



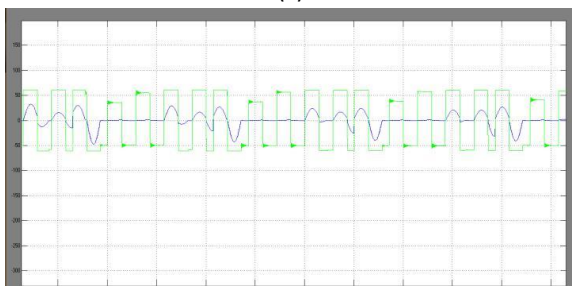
(a)



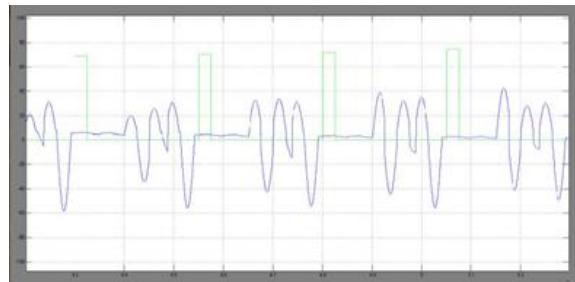
(b)



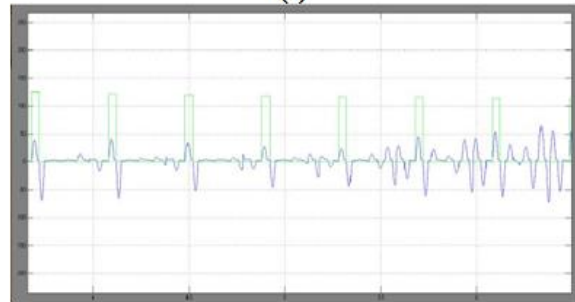
(c)



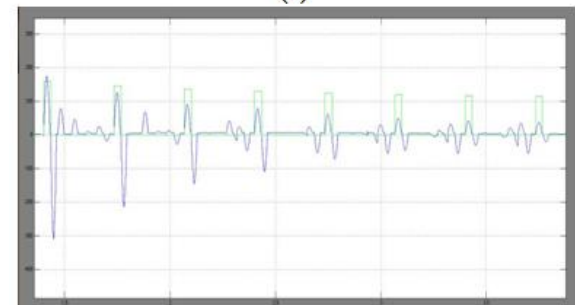
(d)



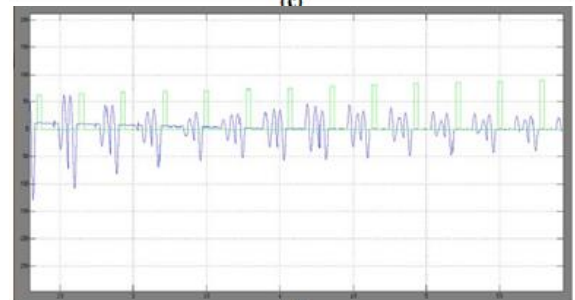
(a)



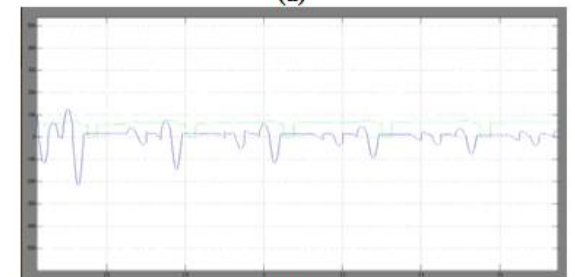
(b)



(c)



(d)



(e)

Fig.11. Experimental waveforms under the open-loop condition (X-axis: Time, 20 μ s/div, Y-axis: Magnitude of the rectifier input voltage: 20 V/div, and series current: 5 A/div)(a) 2.5 kHz switching frequency. (b) 3kHz switching frequency. (c) 3.5 kHz switching frequency. (d) 4 kHz switching frequency.

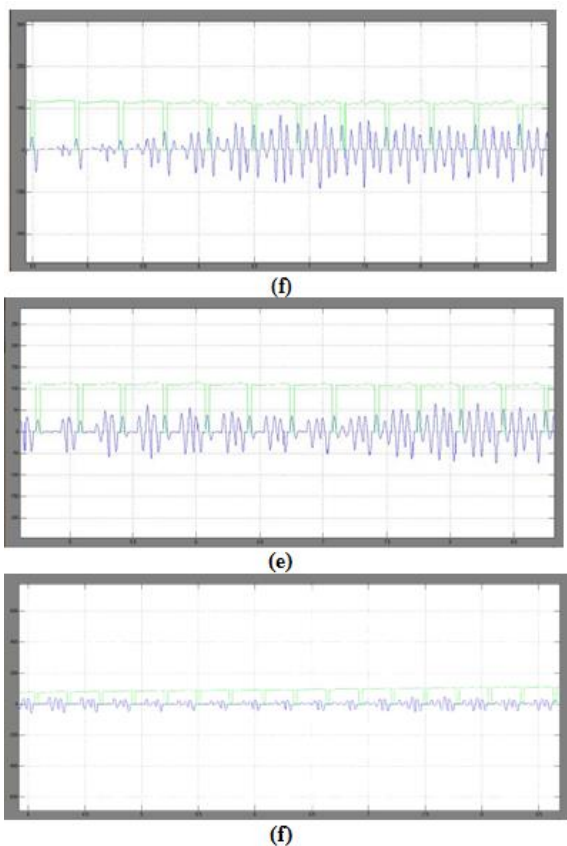


Fig 12. Experimental waveforms of switch voltages in Cell 1 under the open-loop condition (X-axis: Time, 50 μ s/div, Y-axis: Magnitude of the cell switch voltage: 50 V/div, and series current: 5 A/div) (a) Upper switch voltage with 2.5 kHz switching frequency. (b) Lower switch voltage with 2.5 kHz switching frequency. (c) Upper switch voltage with 3 kHz switching frequency. (d) Lower switch voltage with 3 kHz switching frequency. (e) Upper switch voltage with 3.5 kHz switching frequency. (f) Lower switch voltage with 3.5 kHz switching frequency.

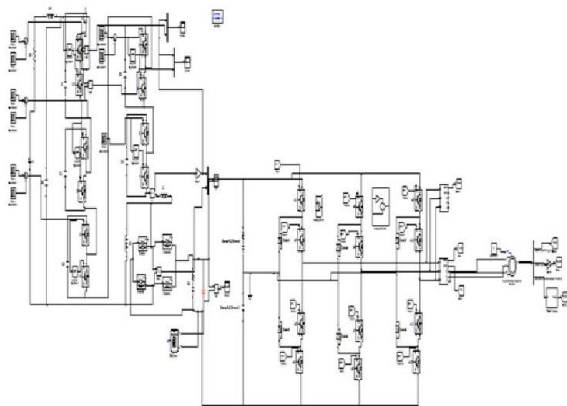


Fig.13. Mat lab/simulation circuit of High step-down ratio

(e) Unidirectional dc-dc converter with Induction Motor.

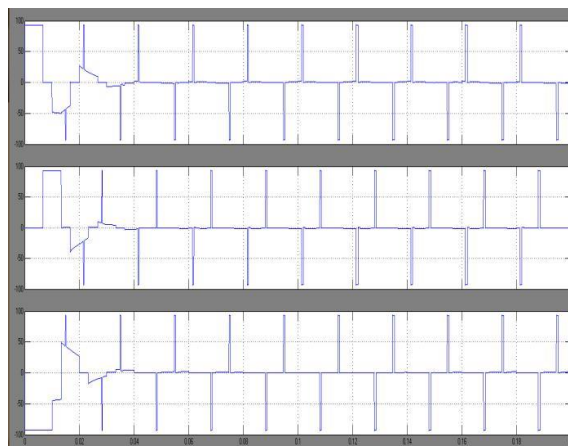


Fig.14. Simulation wave form of output line voltages

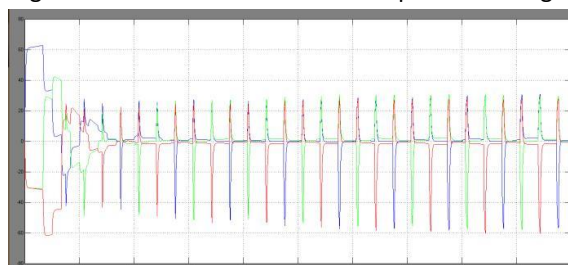


Fig.15. Simulation wave form of output line current

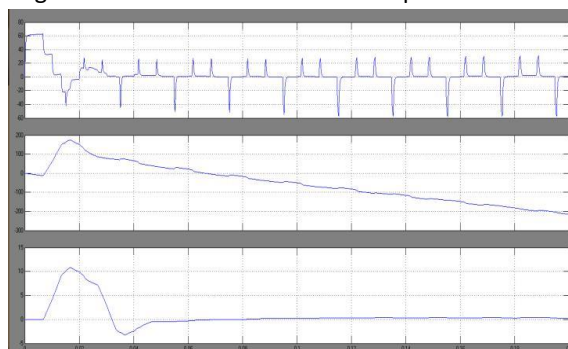


Fig.16. simulation wave form of High step-down ratio unidirectional dc-dc converter with Induction Motor stator current, speed and torque

V. CONCLUSION

As high step-down ratio dc-dc converters become increasingly interesting, there is a strong demand of novel dc-dc converter topologies. This paper has presented a new transformer less MMC dc-dc converter. The dc capacitors of the cells are used also for the resonant operation. The equivalent operating frequency can be increased as a function of the number of half bridge cells and the voltage step-down ratio is also dependent on the number of the cells. The proposed converter has a simple configuration and inherent-balancing capability.

Two resonant operating frequencies exist in the converter. The converter can operate under open-loop control as a dc transformer. It exhibits a good linearity with different switching frequencies. When the closed-loop controller is used for the converter, the capacitor voltages are balanced and the output voltage is regulated within a smaller tolerance range of the rated value. Compared to the other topologies such as PETs, the proposed converter may exhibit more losses as a high ac current is flowing through the cells. However, the proposed converter can eliminate the use of transformers and even cell voltage sensors. Hence, the proposed converter has Induction Motor characteristics and simplicity which may be suitable for high-voltage and low-power applications.

VI. REFERENCES

- [1] M. Hagiwara and H. Akagi, "Control and experiment of pulsewidthmodulated modular multilevel converters," *IEEE Trans. Power Electron.*, vol. 24, no. 7, pp. 1737–1746, Jul. 2009.
- [2] J. Mei, B. Xiao, K. Shen, L. Tolbert, and J. Y. Zheng, "Modular multilevel inverter with new modulation method and its application to photovoltaic grid-connected generator," *IEEE Trans. Power Electron.*, vol. 28, no. 11, pp. 5063–5073, Nov. 2013.
- [3] P. Rodriguez, M. Bellar, R. Munoz-Aguilar, S. Busquets-Monge, and F. Blaabjerg, "Multilevel-clamped multilevel converters (MLC2)," *IEEE Trans. Power Electron.*, vol. 27, no. 3, pp. 1055–1060, Mar. 2012.
- [4] H. Akagi, "Classification, terminology, and application of the modular multilevel cascade converter (MMCC)," *IEEE Trans. Power Electron.*, vol. 26, no. 11, pp. 3119–3130, Nov. 2011.
- [5] K. Ilves, A. Antonopoulos, S. Norrga, and H.-P. Nee, "A new modulation method for the modular multilevel converter allowing fundamental switching frequency," *IEEE Trans. Power Electron.*, vol. 27, no. 8, pp. 3482–3494, Aug. 2012.
- [6] A. Lesnicar and R. Marquardt, "An innovative modular multilevel converter topology suitable for a wide power range," in *Proc. IEEE BolognaPower Tech Conf. Proc.*, Bologna, 2003, vol. 3, pp. 1–6.
- [7] S. Allebrod, R. Hamerski, and R. Marquardt, "New transformerless, scalable modular multilevel converters for HVDC-transmission," in *Proc. IEEE Power Electron. Spec. Conf.*, 2008, pp. 174–179.
- [8] M. Guan and Z. Xu, "Modeling and control of a modular multilevel converter-based HVDC system under unbalanced grid conditions," *IEEE Trans. Power Electron.*, vol. 27, no. 12, pp. 4858–4867, Dec. 2012.
- [9] M. Glinka and R. Marquardt, "A new ac/ac multilevel converter family," *IEEE Trans. Ind. Electron.*, vol. 52, no. 3, pp. 662–669, Jun. 2005.
- [10] L. Baruschka and A. Mertens, "A new three-phase ac/ac modular multilevel converter with six branches in hexagonal configuration," *IEEE Trans. Ind. Appl.*, vol. 49, no. 3, pp. 1400–1410, May/Jun. 2013.
- [11] X. Liu, H. Li, and Z. Wang, "A start-up scheme for a three-stage solid-state transformer with minimized transformer current response," *IEEE Trans. Power Electron.*, vol. 27, no. 12, pp. 4832–4836, Dec. 2012.
- [12] T. Zhao, G. Wang, S. Bhattacharya, and A. Q. Huang, "Voltage and power balance control for a cascaded H-bridge converter-based solid-state transformer," *IEEE Trans. Power Electron.*, vol. 28, no. 4, pp. 1523–1532, Apr. 2013.
- [13] J. Ferreira, "The multilevel modular dc converter," *IEEE Trans. Power Electron.*, vol. 28, no. 10, pp. 4460–4465, Oct. 2013.
- [14] F. Khan and L. Tolbert, "A multilevel modular capacitor-clamped DC-DC converter," *IEEE Trans. Ind. Appl.*, vol. 43, no. 6, pp. 1628–1638, Nov./Dec. 2007.
- [15] D. Cao and F. Z. Peng, "Multiphase multilevel modular DC-DC converter for high-current high-gain TEG application," *IEEE Trans. Ind. Appl.*, vol. 47, no. 3, pp. 1400–1408, May/Jun. 2011.
- [16] Xiaotian Zhang, Timothy C. Green and Adria Junyent-Ferrie, "A New Resonant Modular Multilevel Step-Down DC-DC Converter with

Inherent-Balancing” IEEE Transactions On
Power Electronics, vol. 30, no. 1, jan 2015.

A Brief bio of Authors

J.V.S.E NARASINGA RAO currently pursuing his M.Tech degree in Power Electronics from Sri Venkateswara Engineering College Suryapet Affiliated to JNTU Hyderabad. His areas of interest are Power Electronics and Renewable Energy Sources.

B. Venugopal Reddy, Received B.Tech degree in Electrical Engineering from JNTU Hyderabad in 2007. M.Tech in Power Electronics from JNTU Hyderabad in 2012. And currently he is pursuing his Ph.D in KL University. Presently he is working as an Associate Professor in EEE dept .at Sri Venkateswara Engineering College, Suryapet. His research area includes Power Systems, Power Converters and Renewable Energy Sources.
